The Tasman Box

Prepared for Deep South

November 2020

Prepared by:
Phil Sutton
Denise Fernandez
Helen MacDonald
Melissa Bowen

For any information regarding this report please contact:

Phil Sutton
Physical Oceanographer

+64-4-386-0386
Phillip.Sutton@niwa.co.nz

National Institute
of Water & Atmospheric
Research Ltd (NIWA)

301 Evans Bay Parade
Hataitai
Wellington 6021
Private Bag 14901
Kilbirnie
Wellington 6241

Phone +64 4 386 0300

NIWA CLIENT REPORT No: 2020328WN
Report date: November 2020
NIWA Project: C01X1412

Quality Assurance Statement		
	Reviewed by:	Graham Rickard
	Formatting checked by:	Alex Quigley
	Approved for release by:	Alison MacDiarmid

Contents

Figures

Executive summary

The western subtropical Pacific Ocean largely determines New Zealand's interannual climate variability, because New Zealand lies downstream of this region in terms of both the atmosphere with its prevailing westerly winds and the ocean with its southward and eastward flowing boundary currents.

The region to the north and west of New Zealand is relatively-well measured by oceanographic standards, with 0-800m temperature measurements collected since the early 1990s using expendable probes deployed from container ships along transects between Sydney and Wellington, Auckland and Fiji, and Fiji and Brisbane. Since 2004 Argo floats have made measurements of temperature and salinity between the surface and 2000m.

There was strong warming in the region in the 1990s that has been reported in earlier publications. Since 2000, changes have been more subtle, but two signals have been identified in this period. The first is in regard to sea level. Sea level changes result from two components. The first is called 'steric height' and is a result of the thermal and haline expansion of water. Warmer and fresher water is less dense and so stands taller. The second term is called 'mass' and is the addition of land-based water into the ocean coupled with large-scale redistribution of water. Satellite products indicate that there is strong sea level rise in the north Tasman Sea at about 5mm/yr since 2000, stronger than the global average of 3.8mm/yr. Steric height typically accounts for one third to a half of sea level change, but in this region the measurements of temperature and salinity indicate the steric trend is only ~1mm/yr. This means the sea level trend due to mass is ~4mm/yr, which is very large by global standards. This is presumably a result of water converging in the region, i.e. water effectively piling up.

The second interesting signal is interannual variability in salinity. It has only been possible to study salinity variability since the establishment of the global Argo array in 2004. Upper ocean salinity changes are caused by changes in the difference between evaporation (E) and rainfall (precipitation, P) or (E-P) as well as through the advection of water with different salinities into a region. Analyses show that both (E-P) and advection are important in determining the upper ocean salinity in the north Tasman Sea. The salinity changes are large enough to impact interannual density variability, which is normally determined almost entirely by temperature. Upper ocean density has an important impact on climate, with denser surface water associated with deeper winter mixed layers and with increasing formation of a water mass called Subtropical Mode Water (STMW). As STMW subducts into the deeper ocean it sequesters heat and carbon dioxide, providing a feedback into the global climate system.

1 Introduction

The temperature of the Tasman Sea largely determines New Zealand's air temperatures because New Zealand lies downstream of this region in terms of both the atmosphere with its prevailing westerly winds and the ocean with its southward and eastward flowing boundary currents. The Tasman Sea heat content is in turn set by the temperatures and speeds of currents flowing into and out of the region together with the local air-sea heat fluxes. Warm, subtropical water flows into the area in the East Australian Current and flows out in the Tasman Front and East Auckland Current. The relative transports of these current systems determine whether warm water converges in or is removed from the region.

This region provides a unique opportunity because it has been sampled ~4 times per year since the late 1980s using expendable bathythermographs (XBTs) deployed from container ships along three routes: between Auckland and Fiji, Fiji and Brisbane, and Sydney and Wellington. This ship routes enclose an area called the Tasman Box. This effort is a collaboration between Scripps Institution of Oceanography, CSIRO and more recently, NIWA (e.g., Sprintall et al 1995, Roemmich et al 2005). Information about the interior of the box is available from satellite measurements of sea surface temperature (SST) and sea surface height (SSH) since 1981 and 1992 respectively, and from measurements of the top 2km of the ocean by Argo profiling floats since 2003. Combining these data allows investigation of the mechanisms changing the heat content of the Tasman Sea.

The Tasman Sea upper ocean temperature has a strong influence on New Zealand's air-sea climate system. The increasing heat content of the Tasman since the 1990s has resulted in a significant sea level rise due to thermal expansion of seawater. In addition, Marine Heat Waves (MHWs) are becoming of increased interest because of their impact on weather, ecosystems and fisheries and recent work has found a link between intensity and occurrence of MHWs and ocean heat content.

This report uses all available data to describe interannual and decadal variability in the Tasman Sea and, where possible, to describe the forcing mechanisms.

The large-scale physical oceanography of the region is dominated by boundary currents (Figure 1-1, from Chiswell et al 2015). The strong and variable East Australian Current (EAC) flows south along the east coast of Australia before separating from the Australian continental shelf in an eddy field at about the latitude of Sydney (e.g., Ridgway and Dunn 2003). Some of the separated EAC water flows across the Tasman Sea to north of Cape Reinga as the Tasman Front (Stanton 1979; Sutton and Bowen 2014). Recent improvements in model and data resolution have indicated that the Tasman Front appears instantaneously as an eddy field (Oke et al 2019) although there remains a defined eastward flow in temporal means.

North of Cape Reinga, the current attaches to the New Zealand landmass, flowing down the northeast coast of the North Island as the East Auckland Current (EAUC) (e.g. Stanton et al 1997). This instance of a separated western boundary current reattaching to a landmass is unique.

While these current systems appear continuous in schematics such as Figure 1-1, the reality is much more complicated, with each of the components having variability as large as the mean, i.e., the flows can occasionally disappear or even reverse. The EAC, Tasman Front and EAUC are dominated by eddies, with some of these eddies being permanent (Roemmich and Sutton 1998, Ridgway and Dunn 2003). The currents also extend to different depths, with the EAC typically being ~1000m deep

(Sloyan et al 2016), the Tasman Front ~800m (Sutton and Bowen 2014) and the EAUC extending to 2000m (Stanton et al 1997).

Recent modelling work (Behrens et al. 2019) indicates that the variability in upper ocean temperatures in the Tasman Sea results from changes in the relative inflows and outflows along its northern edge, that is changes in the EAC inflow and EAUC outflow. This indicates that the interplay between these currents determines the conditions in the Tasman Sea that in turn determine New Zealand's climate.

There is also a climatically significant watermass formed in the Tasman Box region, with the north Tasman being an area of Subtropical Mode Water (STMW) formation (Fernandez et al., 2017). STMW is formed when deep winter mixed layers create a layer of 14-20°C water which is then capped by seasonal warming in spring. The subsurface water subducts into the thermocline effectively sequestering heat and CO_2.

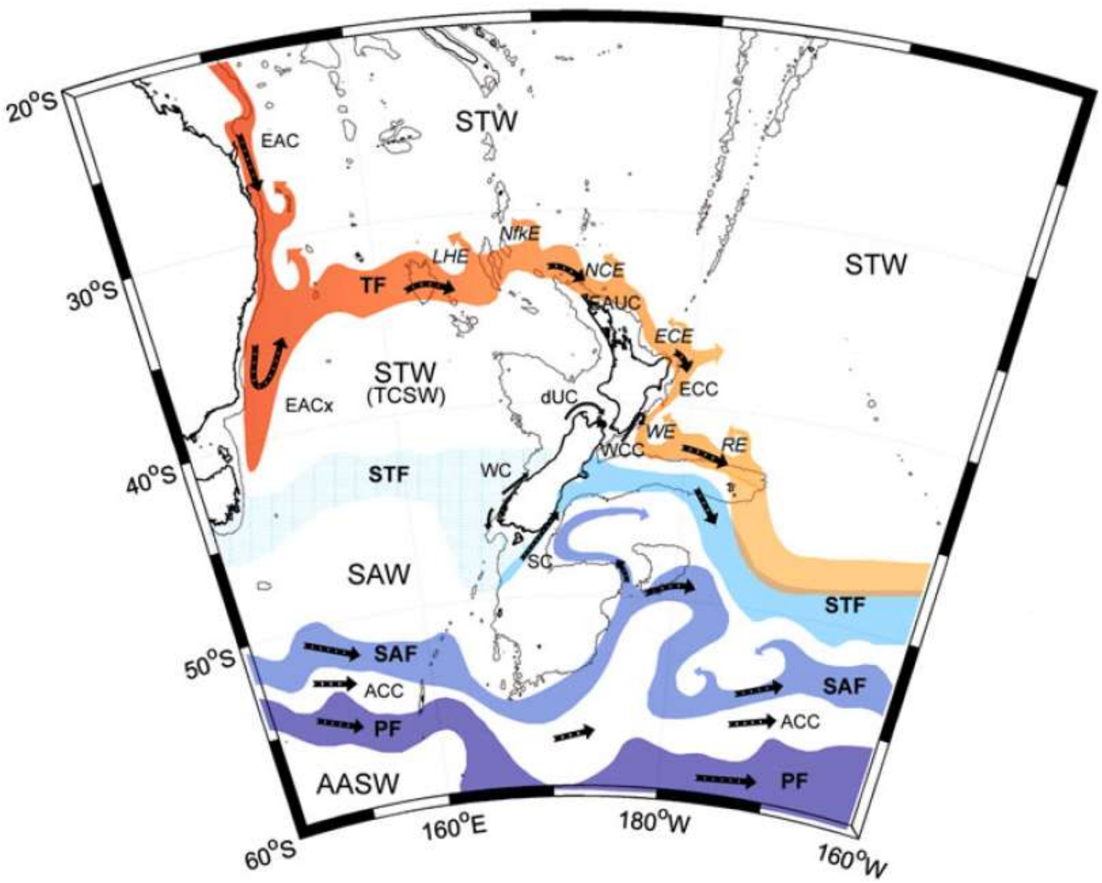

Figure 1-1: (From Chiswell et al, 2015). Schematic surface circulation around New Zealand based on drifter and hydrographic data. Regions of flow are shown as coloured streams. Colours reflect the temperature of the flows with red being warmest, and dark blue being coldest. The STF in the Tasman Sea is density compensated with little flow, as indicated by the shading. Water Masses are Subtropical Water (STW), Tasman Sea Central Water (TSCW), Subantarctic Water (SAW) and Antarctic Surface Water (AASW). Ocean fronts are Tasman Front (TF), Subtropical Front (STF), Subantarctic Front (SAF) and Polar Front (PF). Ocean currents are East Australia Current (EAC), East Australia Current extension (EACx), East Auckland Current (EAUC), East Cape Current (ECC), d'Urville Current (dUC), Wairarapa Coastal Current (WCC), Westland Current (WC), Southland Current (SC) and Antarctic Circumpolar Current (ACC). Eddies are Lord Howe Eddy (LHE), Norfolk Eddy (NfkE), North Cape Eddy (NCE), East Cape Eddy (ECE), Wairarapa Eddy (WE) and Rekohu Eddy (RE).

2 Data

2.1 Expendable Bathythermograph: XBT

The longest timeseries of subsurface ocean temperatures in the southwest Pacific are along transects between Sydney and Wellington, Auckland and Fiji, and Fiji and Brisbane which have been measured from the surface down to 800 m depth roughly four times per year since 1991. These sections are the World Ocean Circulation Experiment (WOCE) repeat high resolution XBT (HRXBT) lines PX34, PX06 and PX30 (http://www-hrx.ucsd.edu/). The measurements are made from ships of opportunity (container ships) using XBTs and have a horizontal resolution of 10–15 nautical miles (17–25 km), with higher resolution through the areas near the coastlines and the boundary currents. There are occasional gaps in the timeseries caused by vessel availability issues and equipment failures, and there is variability in the precise ship tracks.

The data were made available by the Scripps High Resolution XBT programme (www-hrx.ucsd.edu). The raw sections consist of profiles of temperature with 2 m vertical resolution. The individual HRXBT sections were initially objectively mapped onto a regular grid at spacing of 0.1° in latitude (PX06) or longitude (PX34) by 10 m in depth, using the procedure described by Roemmich (1983). This mapping process is designed so the shallowest data are associated with 5 m depth, avoiding errors associated with XBT technical issues in the upper 2.5 m of the water column. Next, the spatially gridded sections were mapped onto a regular temporal grid using a least-squares harmonic analysis technique as described in Sutton and Roemmich (2001) and Sutton et al. (2005) (modified from Roemmich and Cornuelle 1990). This technique is more complicated than, for example, linear interpolation, but is necessary because the approximately quarterly sampling barely resolves the annual cycle. The harmonic analysis directly calculates the seasonal cycle using the full timeseries, thereby enabling harmonic interpolation through years with insufficient temporal resolution to resolve the annual cycle.

The harmonic analysis was set up such that the shortest period fitted was 6 months, and the longest was 60 years. In addition, as in Sutton et al. (2005), a mean and linear trend were fitted to the data at each grid point and then removed before the remaining anomalies were interpolated. A random error of 0.2°C was assumed for the XBT measurements to account for both errors in the temperature measurement and errors in the fall rate (Georgi et al. 1980; Roemmich and Cornuelle 1990). The harmonic analysis has an associated power spectrum related to the amplitudes of the harmonics. The a priori power spectrum was defined as a function of depth and frequency, with an e-folding scale with depth chosen to be 200 m (e–z/200), reflecting observed decaying variability with depth, and a red frequency dependence. Spectral peaks were added at the annual and semi-annual cycle with amplitudes based on the seasonal variability in the data and with vertical e-folding scales of 200 m, to account for the upper ocean seasonal cycle and its asymmetry. This a priori power spectrum was developed to be consistent with the spectral behaviour of the data. The red spectrum lowers high-frequency responses, allowing the interannual variability to be focused on, and limits spurious behaviour in data gaps. The data minus fit residuals were consistently less than 1 standard deviation. The result of the interpolation and harmonic analysis is a regularly gridded temperature product in space and time.

XBTs are simple instruments. The temperature is measured by a thermistor with an accuracy of ± 0.2°C while the depth of the measurement is calculated using a fallrate equation with errors of the order of 2% of depth or 5 m. Considerable efforts have been made to understand and improve XBT data by correcting for biases and fall rate errors, which have both been found to vary with probe type and time of manufacture (e.g. Cowley et al. 2013; Cheng et al. 2014). The errors are mitigated in this analysis because all of the probes used are of the same type (Sippican Deep Blue) deployed from similar platforms (container ships). In addition, the temperature and fall rate coefficient biases have been relatively constant since 1987, i.e. through the time period of these measurements (Cheng et al. 2014). Finally, the results presented here are based on anomalies, thereby removing the impacts of time-mean biases. For these reasons, we have not applied time-dependent corrections, but chosen the approach of using the Hanawa et al. 1995 fall-rate equation followed by the horizontal and temporal objective analyses, analogous to previous analyses of these data (e.g. Roemmich and Cornuelle 1990; Sutton and Roemmich 2001; Sutton et al. 2005).

The timeseries of temperature changes in the eastern Tasman Sea along part of the px34 line between Sydney and Wellington is shown in figure 2-1. Only the eastern portion of the line is shown to avoid the high variability EAC (Sutton et al. 2005).

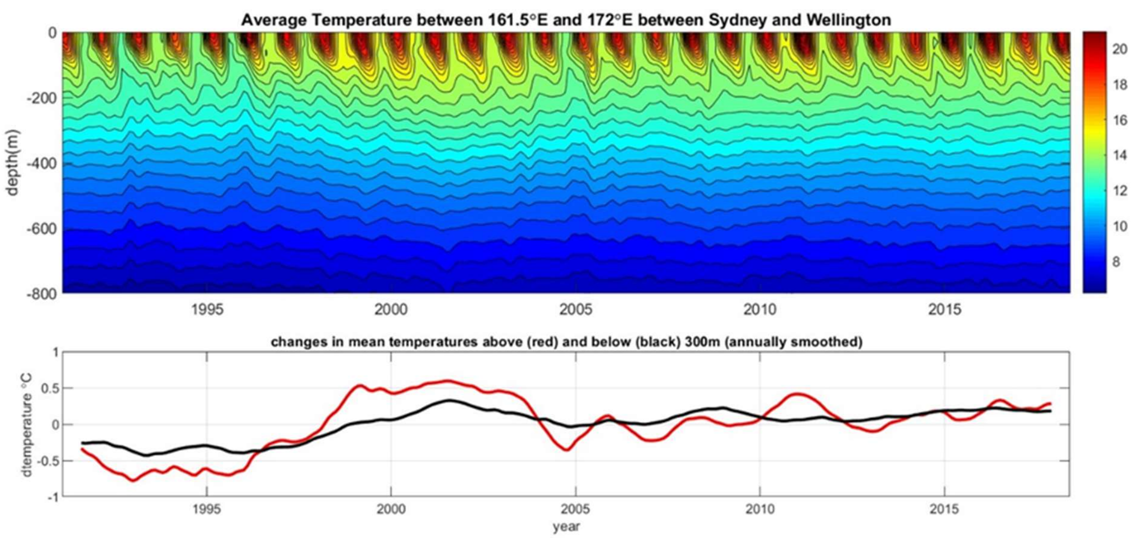

Figure 2-1: Temperature between 161.5°E and 172°E from the PX34 HRXBT transect between Sydney and Wellington. The lower panel shows the temperature changes between the surface and 300m depth in red and between 300-850m in black.

2.2 Argo

Argo is a programme with more than 3500 profiling floats deployed in all of the world's oceans (e.g. Roemmich et al. 1998). Each float typically measures and transmits profiles of temperature and salinity between the surface and 2000 m depth every 10 days, and adequate coverage in the New Zealand region was achieved in 2004. The analyses here are based on the objectively-mapped Argo product from Roemmich and Gilson (2009) (herein the R&G climatology), which uses the nearest 100 Argo profiles to estimate monthly temperature and salinity between the surface and 2000 m at each degree of latitude and longitude from 2004 to the present. The result is a gridded product of temperature between the surface and 2000 m depth with monthly time resolution and 1°latitude/longitude spatial resolution.

Argo profile data are dispersed throughout the region, provide data down to 2000m (compared with 850m for the XBTs) and include salinity. They provide information about the interior of the Tasman Box, complementing the perimeter information from the HRXBT transects, but only since 2004.

The high-quality CTD used on Argo floats combined with rigorous quality control make the Argo data very accurate and mean that the sampling error is larger than measurement errors. Sampling issues around New Zealand are the relatively few floats prior to 2006 and the lack of data in water shallower than 1000m, including over Challenger Plateau. Roemmich and Gilson (2009) compare the objectively analysed Argo surface temperature with satellite sea surface temperature products and find a mean variance of about 0.04°C^2, corresponding to a difference of ~0.2°C.

The regional mean temperature and salinity fields at 10m depth are shown in Figure 2-2. The largest signal in the temperature field is the meridional cooling with increasing latitude, but this zonal pattern is perturbed by the flow field, with isotherms dipping south off the east coast of Australia and east coast of northern New Zealand because of the southward flowing EAC and EAUC.

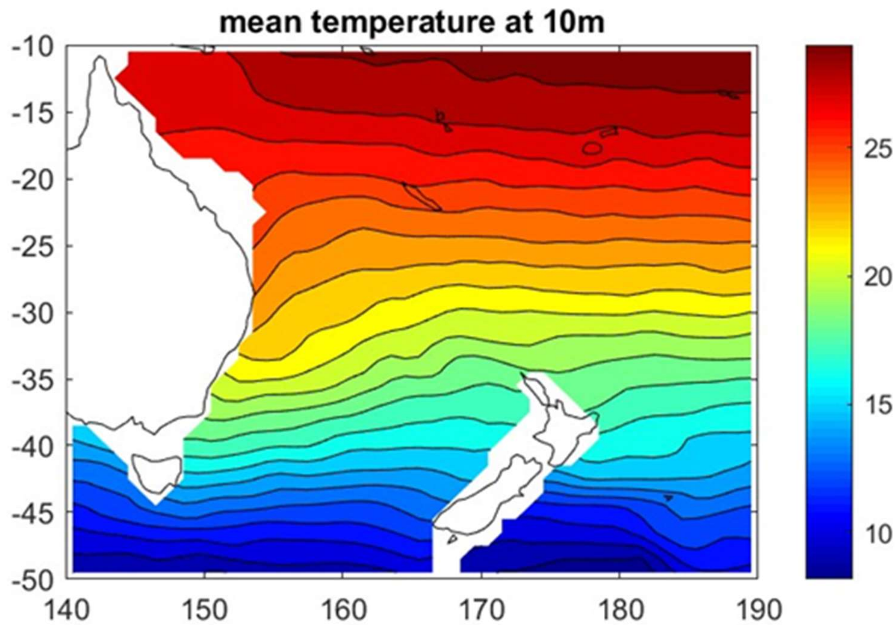

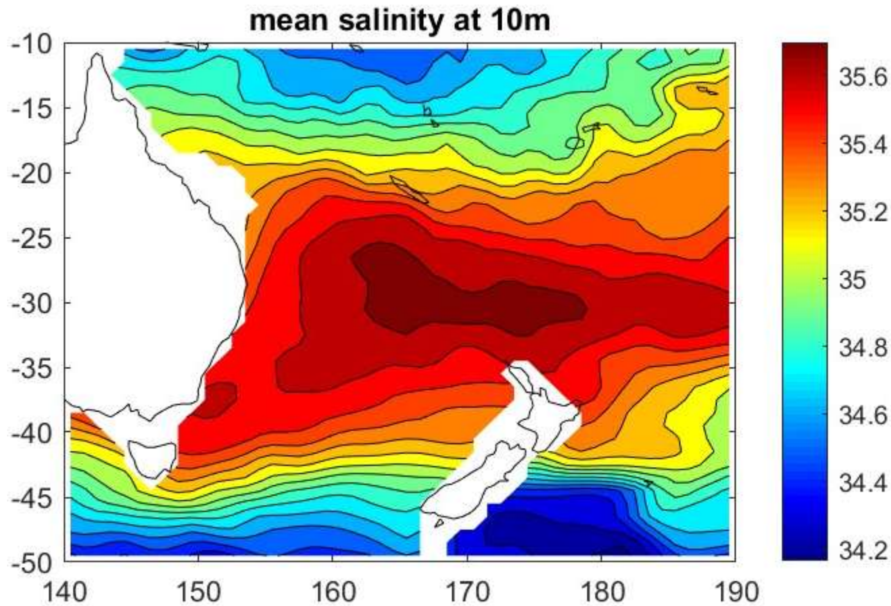

Figure 2-2: Mean temperature and salinity fields at 10m depth from the R&G climatology. The surface salinity distribution is also dominated by the zonal pattern resulting from large scale precipitation and evaporation- with precipitation exceeding evaporation and therefore fresher surface waters in both the tropics and the Southern Ocean separated by a saltier region. Again, the impacts of the boundary currents are clear, with the EAC transporting fresher water to the south, and the EAUC transporting slightly saltier water southward.

2.3 Surface Fluxes

The ERA5 reanalysis heat flux components from the ECMWF Copernicus Data Centre were used to determine the heat flux and evaporation minus precipitation. ERA 5 is the successor of ERA Interim and combines observations which are dynamically consistent with a wide range of atmospheric and oceanic variables. The monthly data has a grid resolution of 0.25˚ in latitude and longitude. Heat, evaporation, precipitation and wind stress fluxes are used in this study (Hersbach et al 2020).

Figure 2-3 shows the mean surface heat flux from ERA5 reanalyses for the Tasman Box and the timeseries of the spatial mean. Negative values mean the ocean is losing heat to the atmosphere.

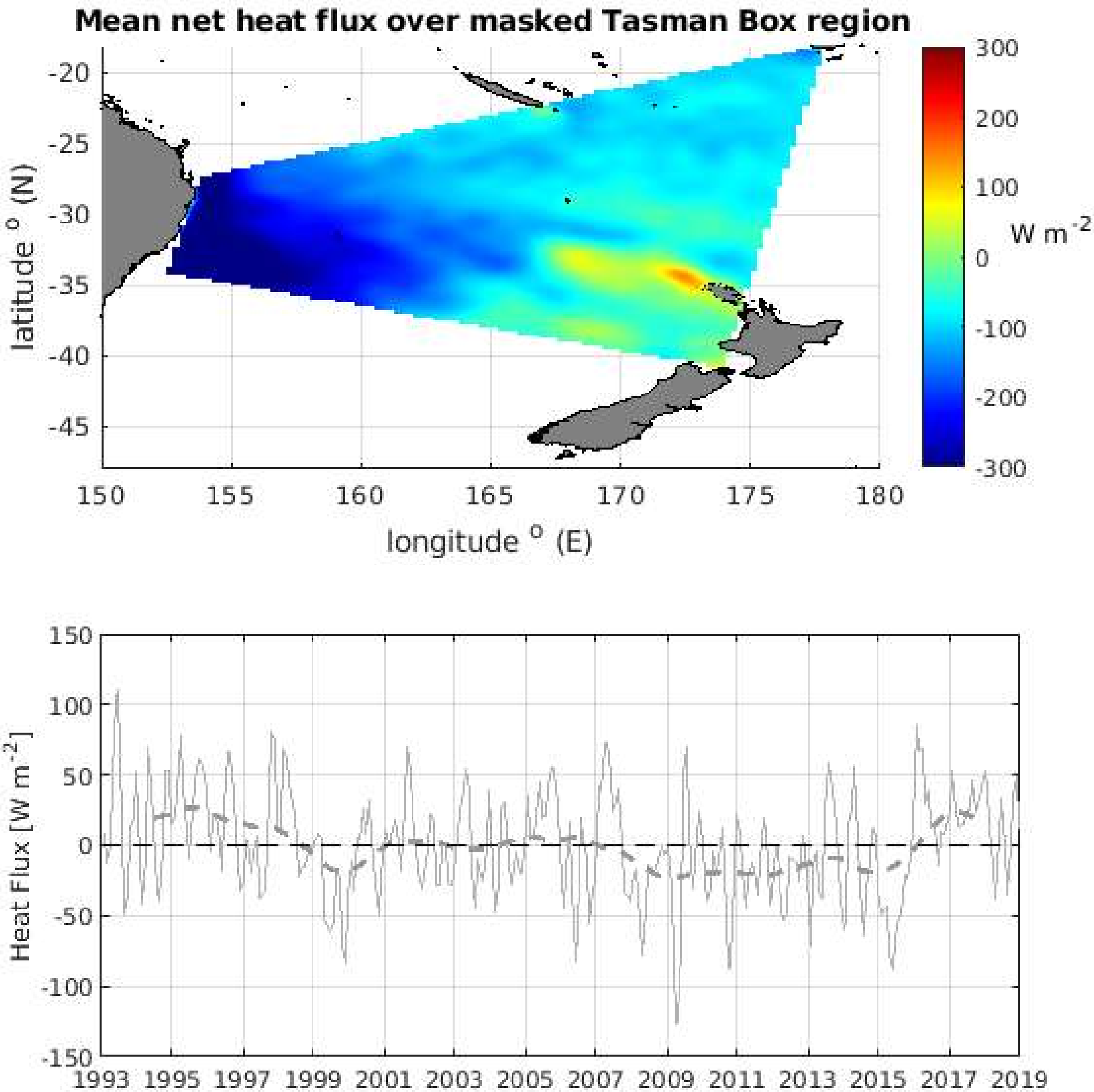

Figure 2-3: Mean surface ERA5 heat flux in the Tasman Box and the timeseries of the areal mean.

Ocean heat uptake is approximately neutral in the Tasman Box. There is a negative area in the western Tasman where the warm, southward flowing EAC loses heat to the atmosphere. Conversely, in the eastern Tasman the atmosphere warms the ocean. There is significant interannual variability with minima in 2000 and 2016, and a prolonged negative period between 2007 and 2013. There is no trend since 1991.

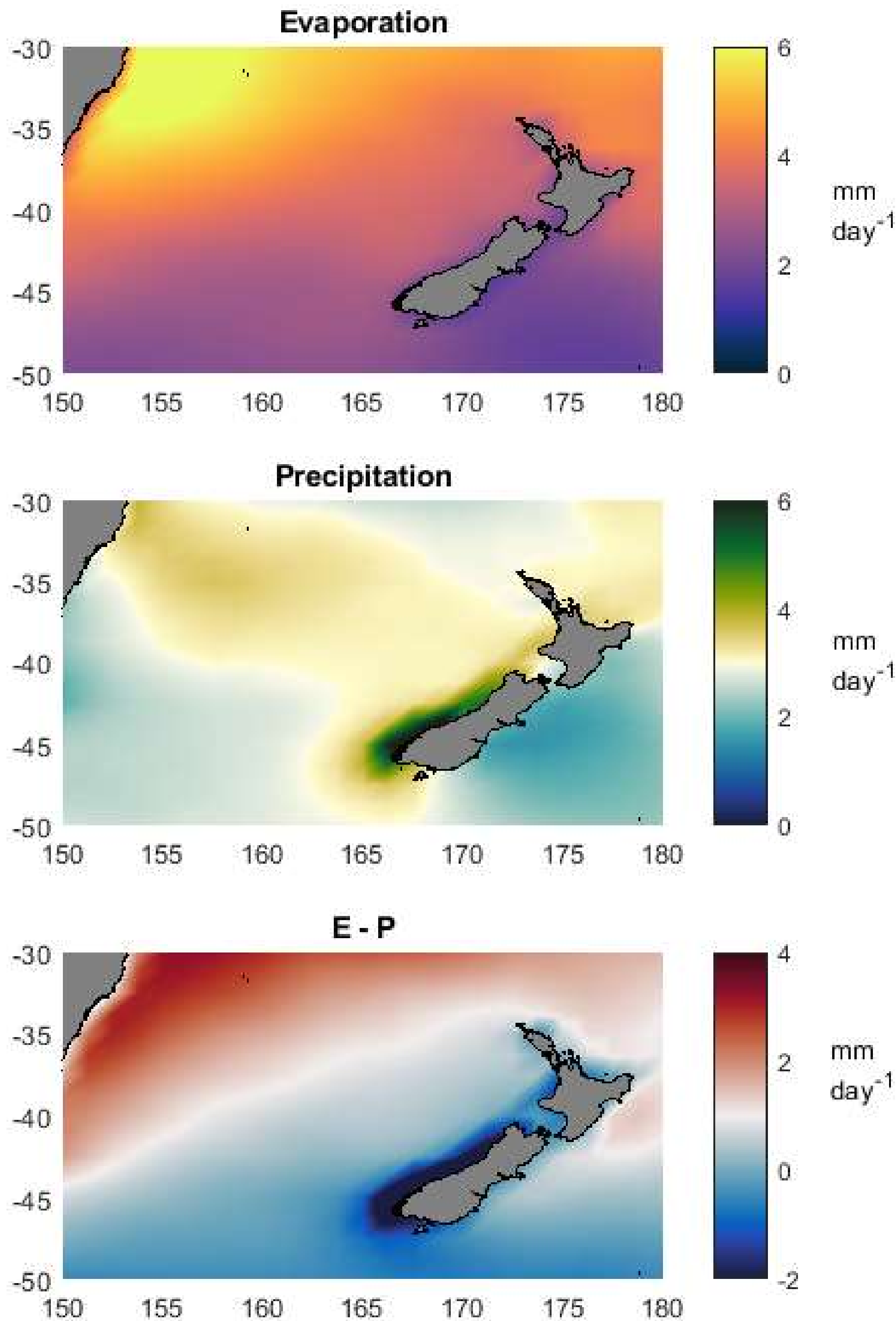

Figure 2-4: Mean evaporation, precipitation and their difference (E-P) over the period 1993-2019 from ERA5.

Evaporation and precipitation are also of interest, with the difference between evaporation and precipitation important in driving upper ocean salinity variability. Spatial mean evaporation, precipitation and their difference (E-P) are shown in Figure 2-4. In the mean, precipitation dominates off the west coast of the South Island. In the central Tasman Sea, the mean E-P pattern resembles that of the mean net heat flux – a NW-SE gradient with evaporation dominating the EAC region where heat loss is the greatest. Focusing on the changes in E-P for the Tasman Box (Figure 2-5) shows higher values in the northwest and lower in the southeast. Over the region there is on average around 2mm/day of evaporation, but significant interannual variability, with low E-P values in 1998 and 2007-2012.

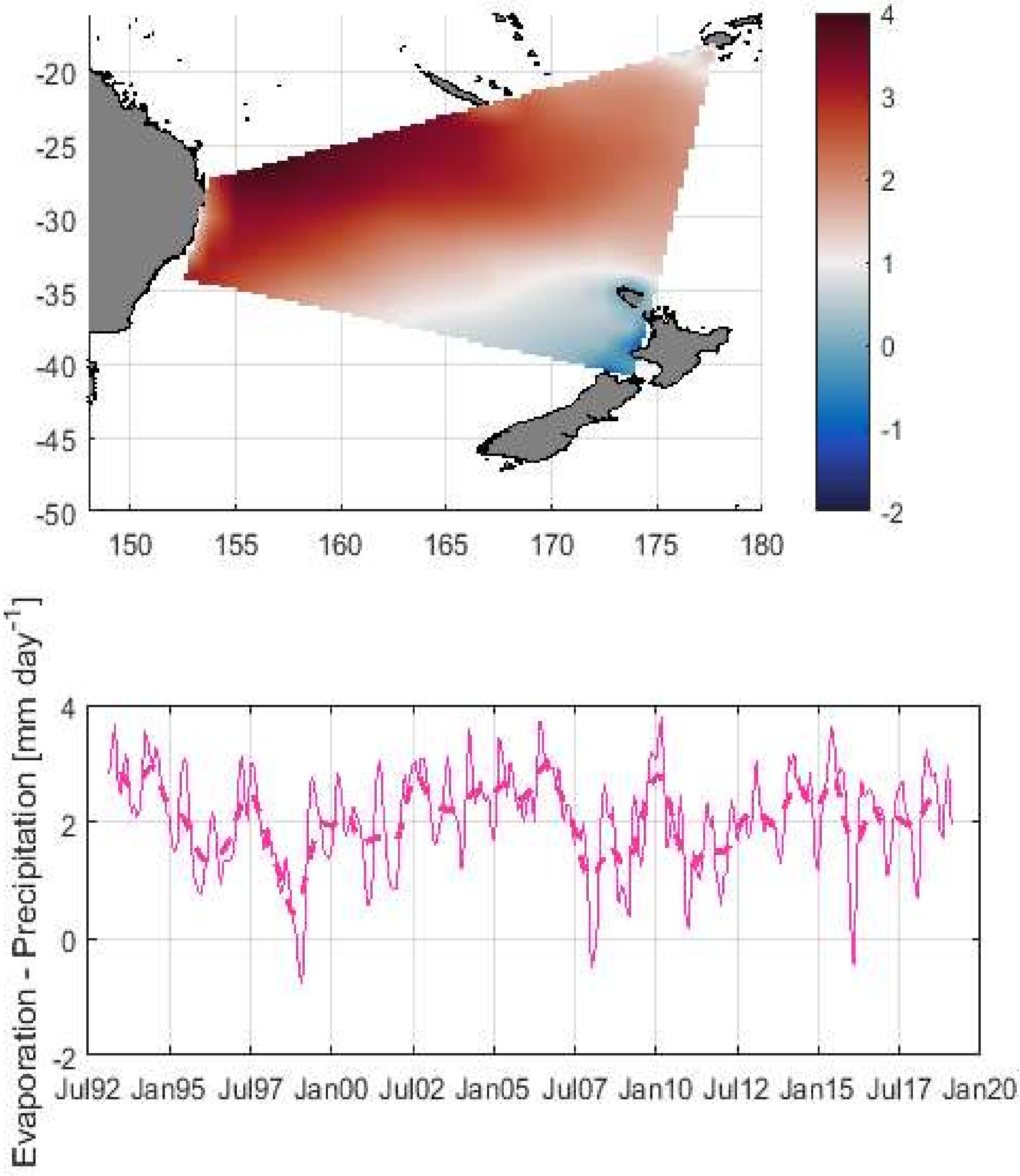

Figure 2-5: E-P from ERA5 for the Tasman Box region. Top is spatial mean, bottom is the time series of the spatial mean.

Changes in wind stress curl (figure 2-6) were also extracted from the ERA5 product. There is significant interannual variability, but no indication of a trend. This is in contrast to decadal trends in windstress curl centred east of New Zealand that have been implicated in spin-up of the South Pacific subtropical gyre (Roemmich et al., 2005; Roemmich et al., 2016).

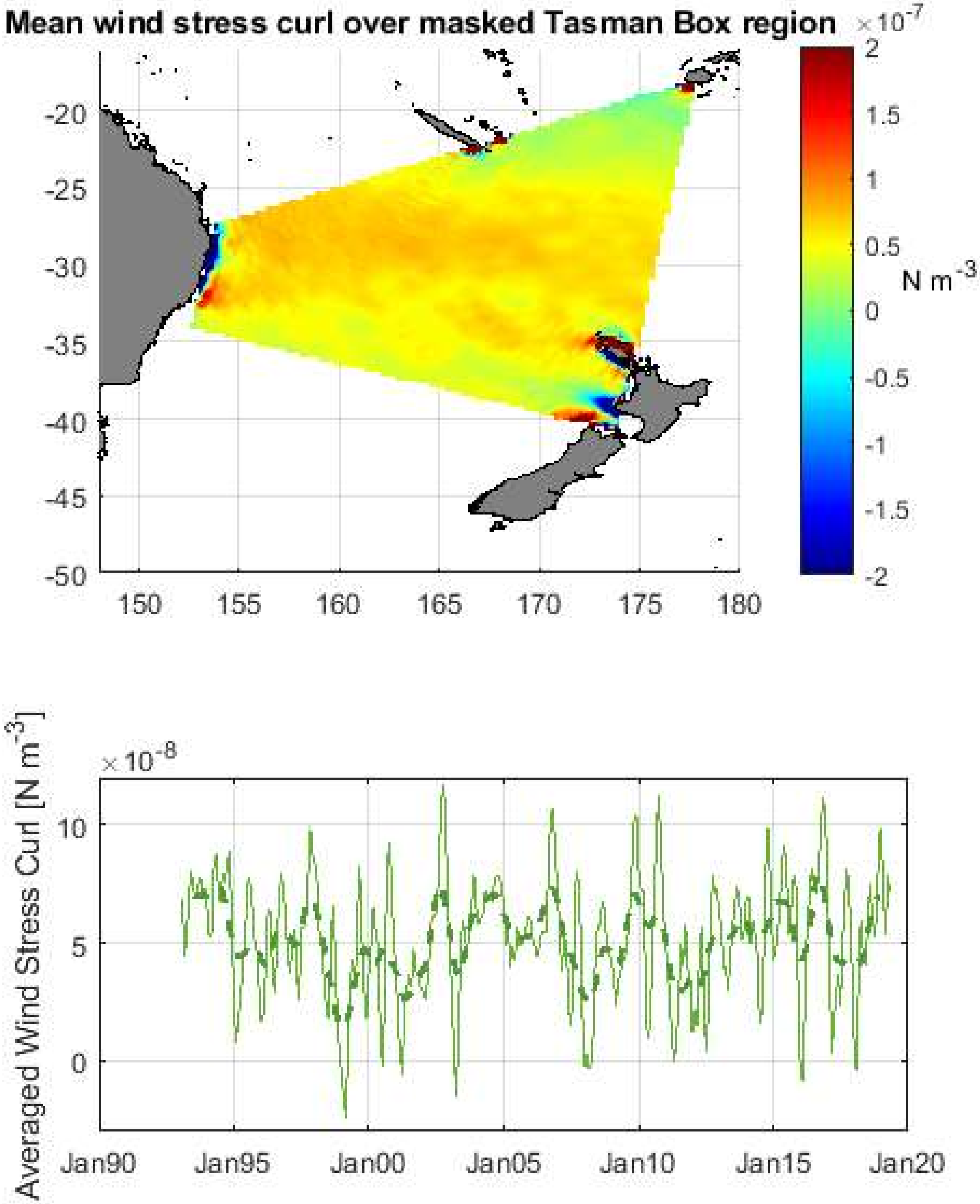

Figure 2-6: Mean wind stress curl for the Tasman Box region from ERA5.

2.4 Satellite sea surface height

Satellite sea surface height data were used for comparison with steric height anomalies and to estimate surface geostrophic transports in the EAC and EAUC following the method of Fernandez et al. 2018. The sea level anomaly (sla) is not directly comparable with steric height, with sla determined by the combination of steric height and mass. Nonetheless, the comparison is useful because steric height accounts for one third to a half of sla long term trends and typically accounts for much of the interannual variability. The products used were AVISO absolute dynamic topography (MADT) and sea level anomaly (SLA) by Ssalto/Duacs and distributed by AVISO with support from CNES (http://www.aviso.oceanobs.com/duacs/) [AVISO, 1998].

2.5 Model O/P.

Output from the CROCO model was compared with measurements of the EAC. The model shows similar mean flows and structure to the measurements. Unfortunately, CROCO is not time-tagged to real time, and so variability can be compared only in a statistical sense.

3 Results

3.1 Argo/HRXBT Comparison

The Argo and XBT temperatures can be compared for the period of overlap. Figure 3-1 shows a comparison of HRXBT and Argo (R&G) estimates of temperature for the eastern Tasman Sea (161.5°E, 166°E, 40°S, 36°S). This is a relatively small area, avoiding Challenger Plateau because Argo floats do not sample on the plateau as it is shallower than the 1000 m Argo parking depth. The eastern Tasman was chosen because it is a relatively uniform and quiescent area which should assist both of the underlying sampling limitations, that is the quarterly XBT sampling and the relatively sparse Argo spatial resolution.

These two independent estimates look largely consistent. The HRXBT result is warmer through 2010 – 2011, probably as a result of there being almost no XBT data along the px34 transect in 2010, with two transects (1003 and 1007) being Sydney to North Cape transects. Figure 3-2 shows the difference profiles.

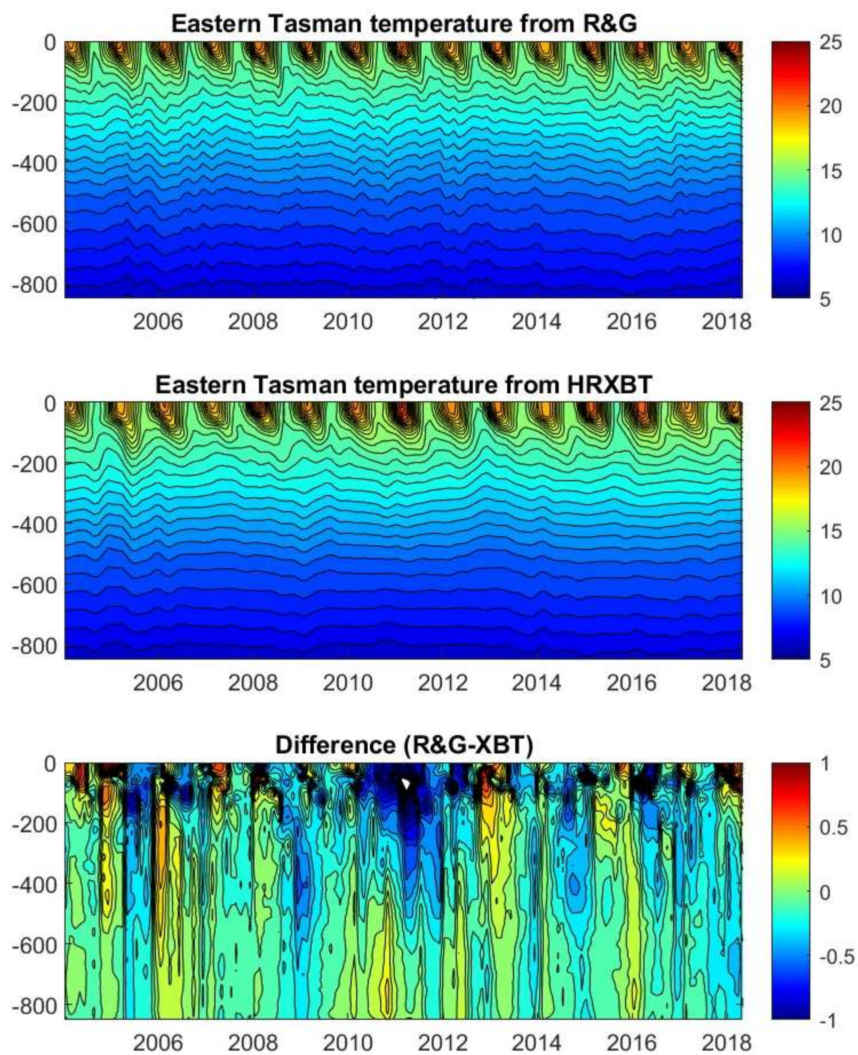

Figure 3-1: Temperature in the eastern Tasman Sea from Argo (Roemmich and Gilson) and HRXBT and their difference.

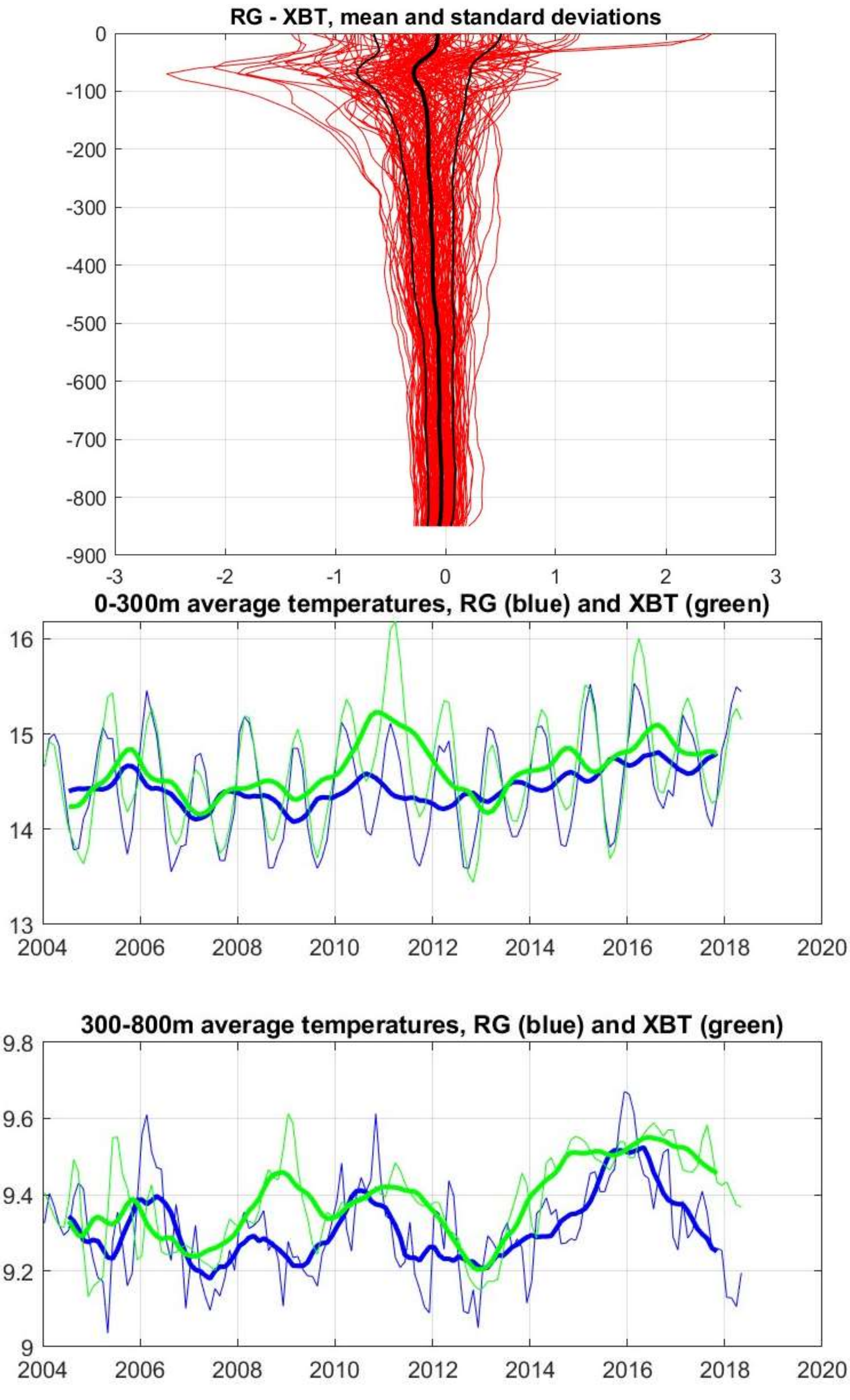

Figure 3-2: Top: Argo (R&G) minus XBT temperatures as a function of depth for the eastern Tasman region (161.5°E, 166°E, 40°S, 36°S) along with the mean difference and standard deviation Centre and bottom: timeseries of mean temperatures from R&G and XBT for depth ranges 0-300m (centre) and 300-800m (bottom), with bold lines being annually smoothed.

Figure 3-2 clearly shows the apparent overestimate in the HRXBT product in the upper 300m in 2010. Beyond that, the agreement is reasonable, but not exceptional. The XBT product is likely compromised by the quarterly sampling and not helped by the relatively crude temperature and depth accuracies. The Argo product should be more accurate, but will not resolve fine spatial scales.

The HRXBT/Argo comparison serves as a warning as to the capabilities of the available data. There have not been strong temperature changes in the area since 2004 (i.e. in the Argo era) unlike those in the 1990s (Sutton et al 2005), and the data may have insufficient signal to noise to describe subtle local interannual variability.

3.2 Temperature and salinity changes

The mean temperature and salinity on the Tasman Box are calculated from the R&G climatology and shown in Figure 3-3. The temperature anomalies are dominated by the annual cycle in the upper 100-200 m, but there is subtle interannual variability, with a slightly cool period 2011-2013, followed by a slightly warm period 2015-2018. The interannual variability in the salinity is more noticeable, made clearer by the absence of an annual cycle. Noticeable in the salinity is a fresh event at the surface from 2008-2013 followed by a salty period. Both of these surface signals subduct into the deeper ocean, with the anomalies reaching at least 400m around 3 years after they began at the surface. The density anomaly indicates that the interannual salinity changes have an appreciable impact on density. This is atypical - in subtropical waters temperature variability normally dominates density changes.

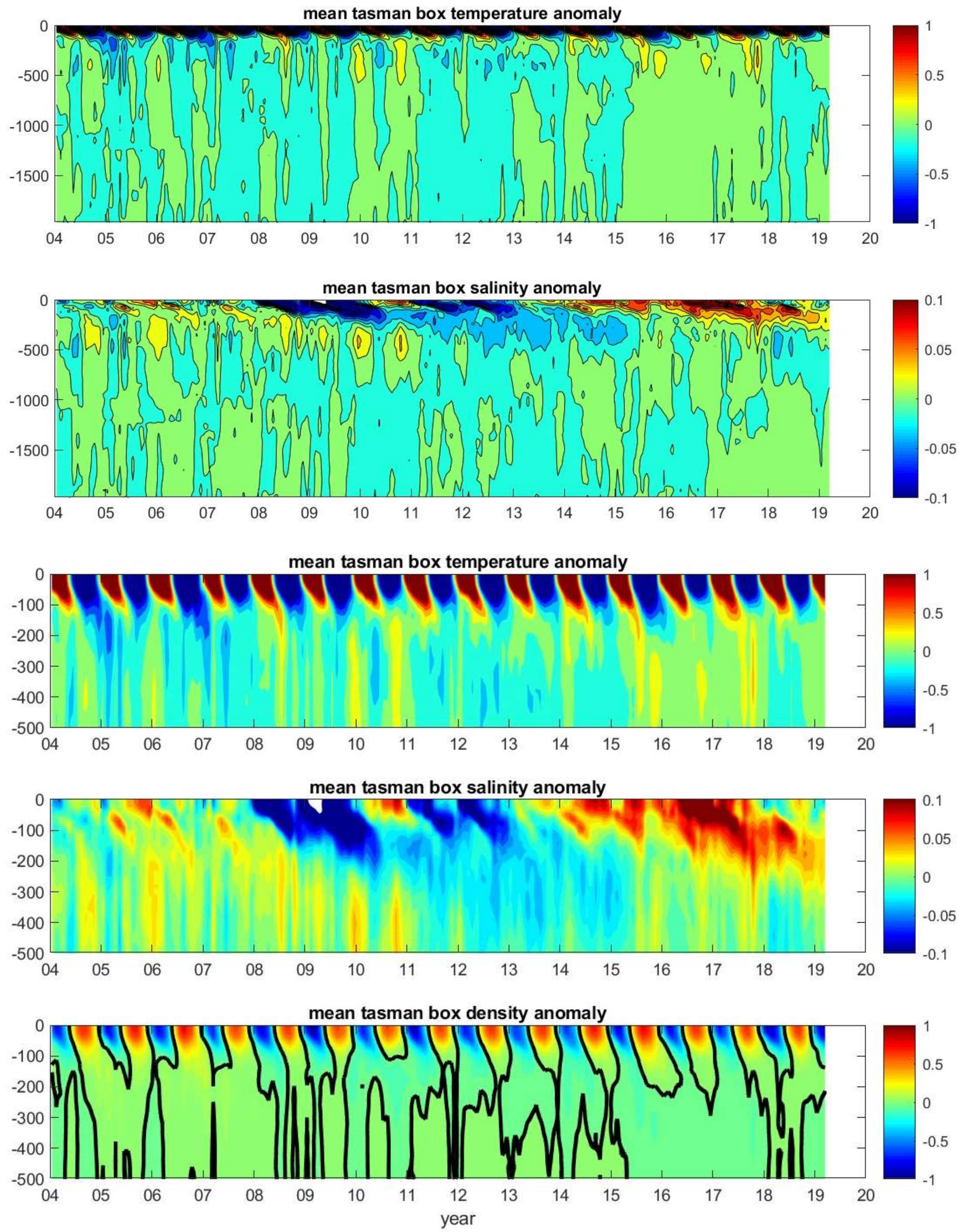

Figure 3-3: Top two panels: Temperature and salinity anomalies between the surface and 2000m. Bottom three panels: temperature, salinity and density anomalies between the surface and 500m. Zero difference contour shown by the bold black curves in lower frame.

Focussing on upper ocean (0-100m) temperature and salinity variability and the resulting changes in density indicates that there have been subtle changes since 2004. The annual cycle dominates the temperature and therefore the density changes but is not of interest, hence annually smoothed parameters are included in figure 3-4. Mean temperature between the surface and 100m has interannual changes of the order of 0.5°C and the suggestion of a warming trend since 2004. Salinity has interannual variability of the order of 0.1-0.2, with no sign of a trend. The change in density for a 0.5°C temperature change is ~0.14 kg/m^3, while for a 0.15 change in salinity, the density change is ~0.11 kg/m^3. Thus, both temperature and salinity changes are roughly equally important in determining the interannual density changes.

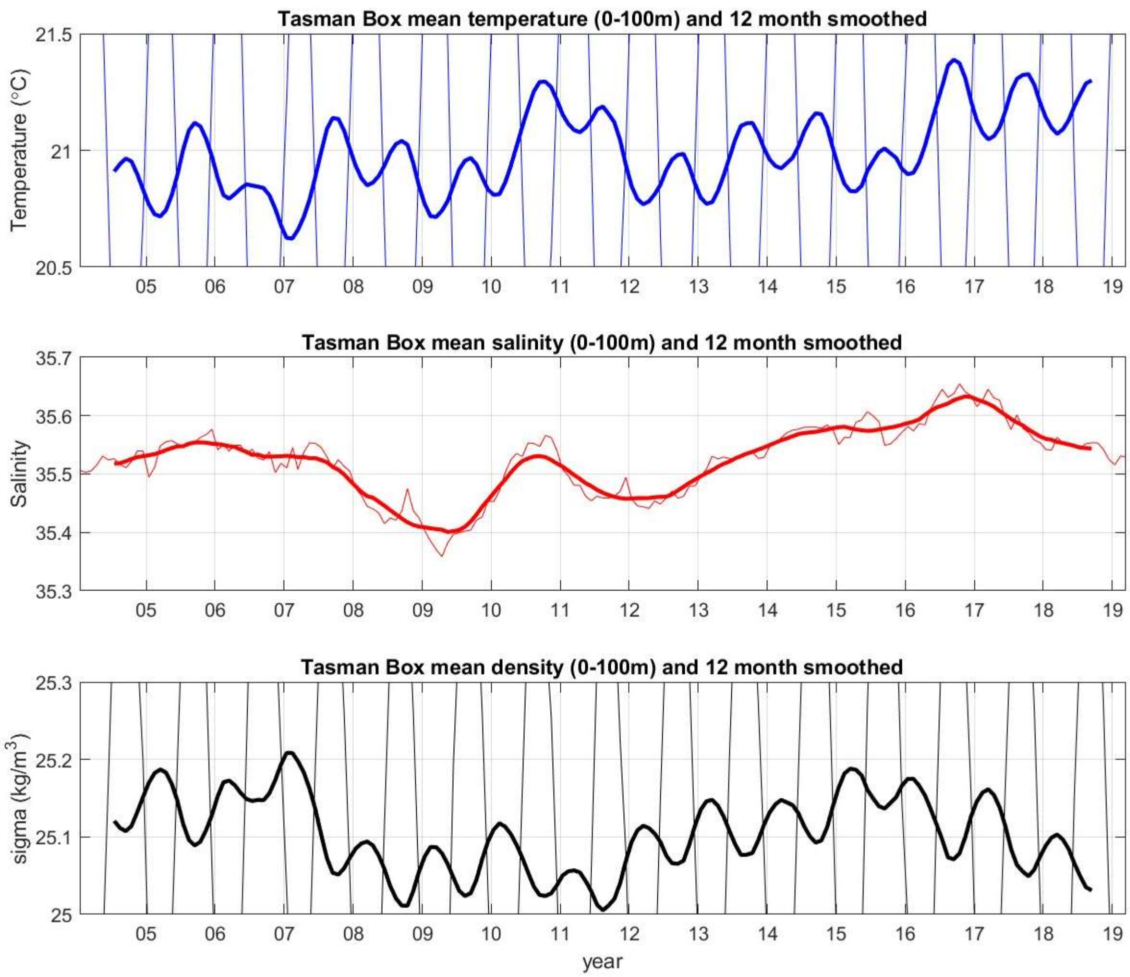

Figure 3-4: Mean Tasman Box 0-100m temperature, salinity and density from R&G climatology. Monthly and annually smoothed.

Upper ocean salinity is determined by the combination of surface fluxes of evaporation and precipitation and horizontal advection. The role of the surface flux term can be evaluated by integrating the freshwater surface flux (E-P) from ERA5 (Figure 3-5). Surface fluxes do appear to have a large impact on upper ocean salinity, but do not explain all the measured changes. The 200-400 mm changes in E-P correspond to mean 0-100 m salinity changes of 0.2, of the order of the variability measured. Figure 3-5 shows the timeseries of the upper 0-100 m salinity and integrated E-P. In the middle panel the impact of E-P is removed- i.e. a 0-100 m salinity is calculated that represents the surface salinity if E-P=0. The inference is that changes in this salinity are caused by advection. The lower panel shows the difference between integrated surface transports in the EAC and the EAUC. Surface EAC water flowing into the Tasman Box is fresher than water flowing out of the box in the EAUC. Thus, positive integrated (EAC-EAUC) should result in upper ocean freshening in the box, while negative integrated (EAC-EAUC) should result in the upper Tasman Box getting saltier. The time series of corrected 0-100m salinity and integrated surface transport difference do show similar variability (figure 3-5, bottom). The conclusion is that both advection and surface fluxes are of roughly equally importance in determining upper ocean salinity.

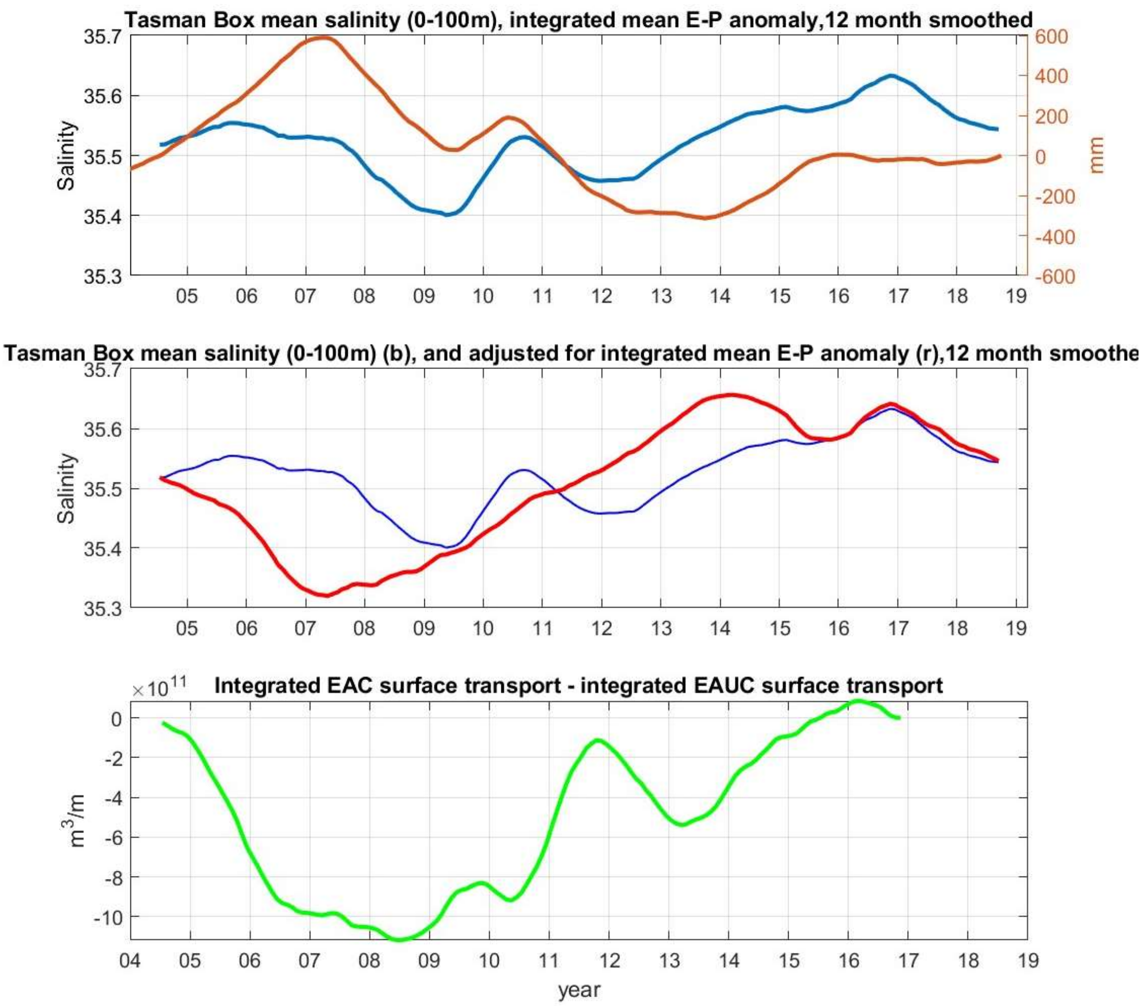

Figure 3-5: Tasman Box mean 0-100m salinity and integrated E-P from ERA5. Middle: mean 0-100m salinity (as in top) and the surface salinity adjusted for E-P: i.e., the salinity that would have been present had E-P been zero. Bottom: the integrated surface transport in the EAC minus the integrated surface transport in the EAUC.

3.3 Steric height and sea level anomaly

A ramification of changes in temperature and salinity is changes in the steric height contribution to sea level because of thermal and haline expansion. Temperature changes have a much larger impact on steric height changes than salinity changes do. The crudest comparison between mean ocean temperature and AVISO sla is shown in figure 3-6 (top) which shows the mean 0-2000m temperature and the mean sla for the Tasman Box.

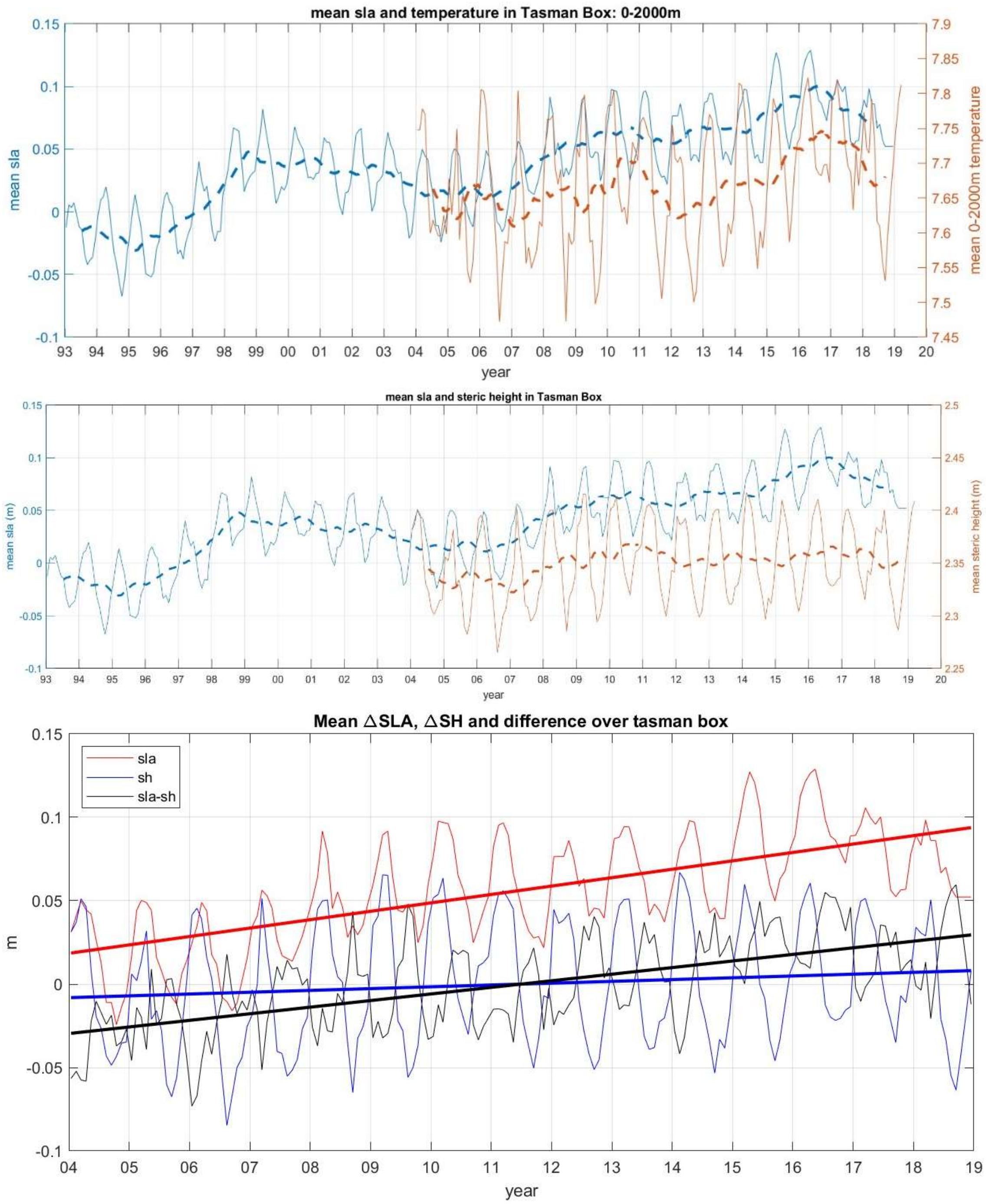

Figure 3-6: Top: mean Tasman Box sla from AVISO (blue) and 0-2000m ocean temperature from R&G climatology (red) with one-year smoothed results also shown. Middle: sla and steric contribution calculated from R&G temperature and salinity. Bottom: sla, steric height and their difference for the Argo period along with linear trends.

Figure 3-6 (middle) shows the steric height changes caused by the 0-2000m ocean temperature and salinity changes together with the mean Tasman Box sla. The annual cycle in steric height (dotted) is larger and not in phase with the annual cycle in sla. This is expected, because the annual cycle in ocean mass has a different phase again, in response to a combination of the interchange of water between being land-based (ice, snow and water) and ocean-based and the asymmetry between the northern and southern hemispheres, with the southern hemisphere having much more ocean area. The interannual variability of the sla and steric height are similar, with the sla variability probably resulting from the steric contribution. The difference term (sla-steric) is an indirect estimate of ocean mass (black lines on bottom panel). Of interest is that the steric trend is almost flat, at 1 mm/yr while there is a significant sla trend of 5 mm/yr. This indicates that there is also a strong trend in ocean mass (4 mm/year). Thus, decadal trends in sea level in the Tasman Box are resulting from increased mass, rather than local heating or freshening. This increased mass must result from ocean convergence, but the current changes corresponding to the convergence are too small to discern from data.

There is a satellite product that estimates ocean mass based on the Gravity recovery and Climate Experiment (GRACE) (e.g. https://en.wikipedia.org/wiki/GRACE_and_GRACE-FO). Globally it has been found that the sea level budget using a combination of sea level from AVISO, steric height from Argo and mass estimates from GRACE closes very well, however locally that is not the case. Attempts to use GRACE to estimate mass in the Tasman Box region did not give credible results, perhaps because of the relatively small ocean area and large topographic changes in the region.

If the transports in and out of the Tasman Box were known precisely, the changing mass in the box would simply be the integral of the difference between incoming and outgoing transports. While we do not have estimates of the full-depth transports along the entire box margins, we do have estimates of the geostrophic surface transports in the EAC and EAUC from AVISO sla data (Fernandez et al 2018). We also know from model analyses that the EAC and EAUC dominate the flow into and out of the area, and in particular that there is little net flow north and south through the Tasman Sea, that is through the southern section (Behrens et al 2019). Figure 3-7 shows the integrated surface transports for the EAC, the EAUC and their difference along with the mass estimated from the difference between sla and steric height. While there are suggestions that these timeseries are sometimes related, any relationship is weak. The simple assumption that the surface transports in the EAC and EAUC capture all of the depth integrated advection around the perimeter of the box is obviously flawed.

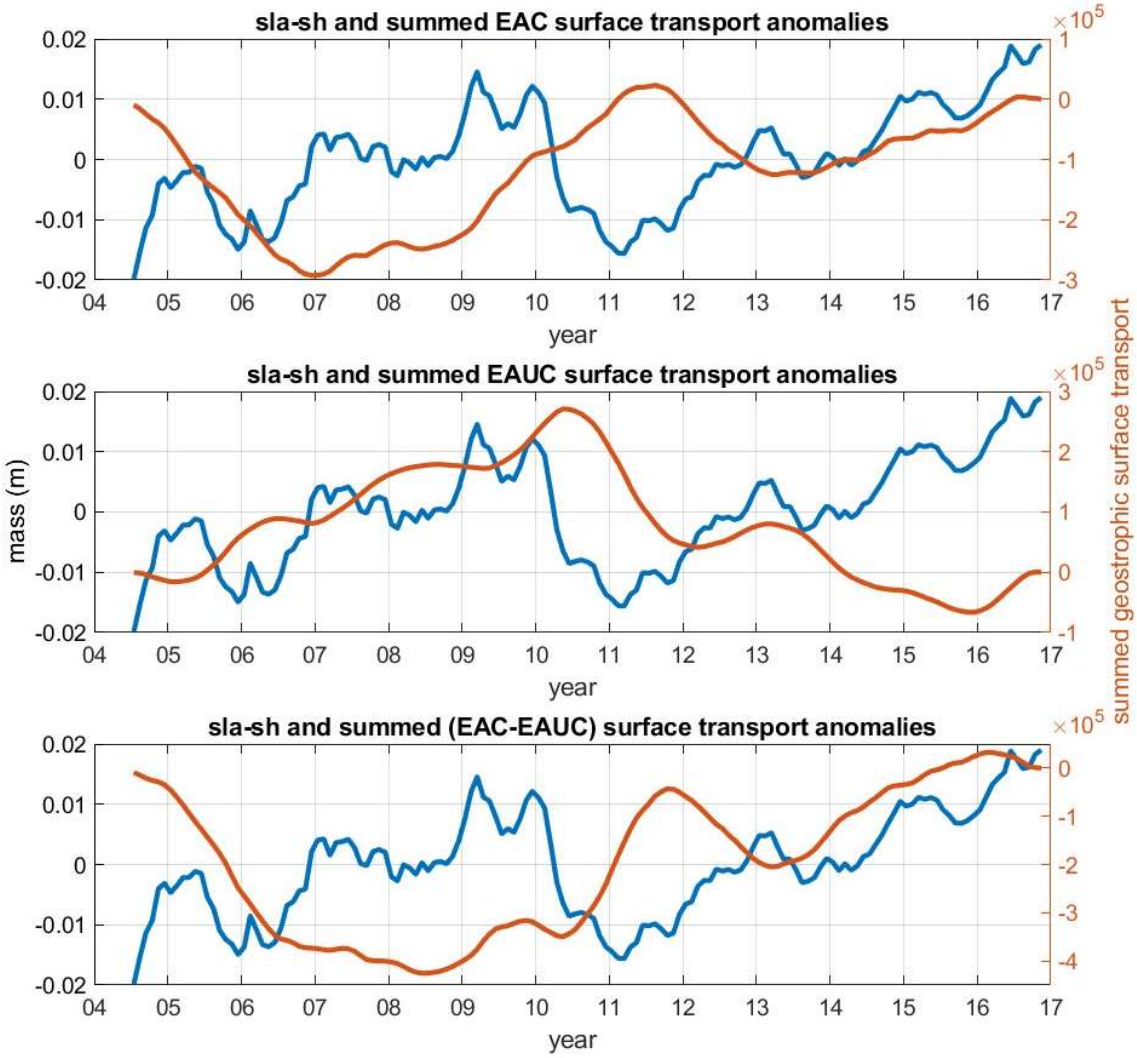

Figure 3-7: Changes in ocean mass estimated from the difference between sea level anomaly from AVISO and steric height from R&G together with integrated surface transports for the EAC, EAUC and their difference calculated from sla gradients across the boundary currents.

3.4 Subtropical Mode Water

Subtropical Mode Water (STMW) is a water mass typically found in each subtropical gyre, formed on the warm side of a western boundary current (WBC). The intense modification of water temperatures in western boundary regions leads to the formation of a lens of homogeneous water that moves away from contact with the atmosphere to a depth between the seasonal and permanent thermocline. Thus, STMW contains a history of ocean-atmosphere interactions and processes influencing the variability of the upper ocean circulation. STMW is characterized by low potential vorticity and minima in the vertical gradients of temperature and density (McCartney, 1982) resulting from weak stratification of the upper layers of the ocean (Hanawa and Talley, 2001). Hence, the term ''mode'' implying that the water mass is relatively thick (Talley, 2011). As with other water masses, the core of STMW forms at the surface (Iselin, 1939) before subducting along isopycnals ventilating the ocean interior where it slowly erodes as it is advected away from its formation region (Hanawa and Talley, 2001; Roemmich et al., 2005; Qiu et al., 2006). All subducted water masses have important global climate implications, because their associated heat and dissolved CO_2 are effectively sequestered for the life of the water mass. Because volumes of STMW are indicators of heat storage and surface temperatures (Dong et al., 2007; Kelly et al., 2010; Rainville et al., 2014) STMW not only plays an important role as a heat reservoir (Hanawa and Talley, 2001) but also preserves a memory of surface conditions at the time the mode water was formed.

The area north of the Tasman Front (figure 1-1) in the Tasman Box is a STMW formation region (e.g. Fernandez et al, 2017), and STMW in this region is often identified as being the water between the 14°C and 20°C isotherms. Variability in STMW formation has been studied in terms of changes in surface fluxes, in particular E-P, and also in terms of boundary layer dynamics. The results here indicate that interannual salinity variability has a similar impact on density variability to temperature variability (figure 3-4), indicating that salinity may be an important modulator for STMW.

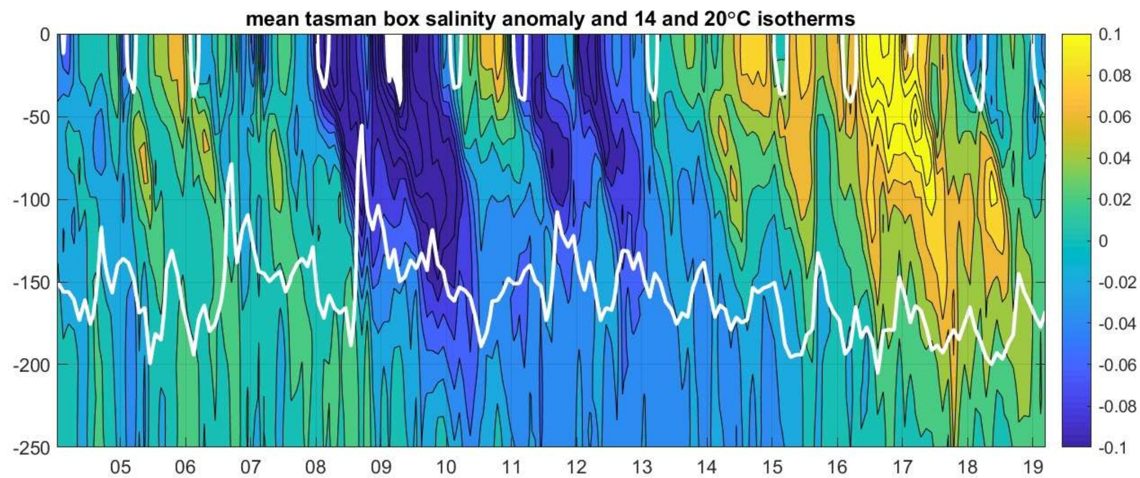

Figure 3-8: The mean Tasman Box salinity anomaly (time and depth) and the depths of the 14°C and 20°C isotherms (white contours).

Figure 3-8 indicates that the shallow salinity anomalies do get subducted into the thermocline and STMW layer (i.e. the area between the two isotherms marked as white lines). There is also a relationship between the thickness of the STMW layer and the salinity, with the fresher salinity anomalies corresponding with a shallower 14°C isotherm and therefore less STMW (2009-2010) and the saltier surface layers corresponding to a deeper 14°C isotherm, that is, a thicker STMW layer (2017-2018). The significant interannual salinity variability in the Tasman Box region that results from a combination of E-P surface fluxes and advection (figure 3-5) modulates the quantity of STMW with climate implications in the form of heat and CO_2 sequestration.

4 Conclusions

The vastly improved data coverage since Argo achieved global coverage in 2004 has coincided with a period of relatively weak changes in the Tasman Sea, making the interpretation of decadal change difficult. Comparison between Argo and XBT temperature data highlight the limitations of the HRXBT data, raising concerns about interpreting subtle changes. However, the significant warming in the Tasman Sea through the 1990s was large enough and well-sampled enough to be unambiguous (Sutton et al 2005).

There are two interesting and not-completely-resolved signals since 2004. The first is a paradox in sea level, with there being a strong trend in sea level rise as measured by satellite, but only a weak increase due to ocean interior density changes. This indicates that there has been a large mass convergence. This mass signal is not apparent in satellite mass estimates, probably because the region is too small and has large bathymetric changes over the scales resolved by the satellite measurements, hampering the calculation of mass from the raw satellite data. We also cannot reproduce a convergence using estimates of the surface flows in the EAC and EAUC based on satellite sla; in this case probably because the subsurface transport variability is too large and uncorrelated with the surface transports. A next direction which is underway is to examine EAC and EAUC transports from a NZESM hindcast (Behrens et al 2019) to ascertain whether the NZESM indicates decadal convergence.

The second interesting signal is the interannual upper ocean salinity variability. Salinity changes have not historically been studied because no suitable timeseries data existed prior to Argo. The occurrence of interannual salinity variability large enough to impact upper ocean density on a level comparable to interannual temperature variability is significant, and will have important implications for upper ocean processes such as mixed layer depth and therefore primary productivity. Salinity variability also appears to have an impact on STMW volume, making it of climate importance. The upper ocean salinity variability results from both local E-P and advection by the EAC and EAUC, with both mechanisms having similar amplitudes. In this case, the surface transports of the EAC and EAUC do appear to be useful in closing the salinity budget - likely because here we are interested in the 0-100m ocean which is better represented by the surface transports than the full-depth transports which contribute to mass.

References

AVISO (1998) AVISO User Handbook: Sea Level Anomaly Files. *CNES Project Document*, AVI-NT-011 312-CN, 3.1st ed. [Available at http://www.aviso.altimetry.fr/fileadmin/documents/data/tools/hdbk_duacs.pdf.]

Behrens, E., Fernandez, D., Sutton, P. (2019) Meridional Oceanic Heat Transport Influences marine heatwaves in the Tasman Sea on Interannual to Decadal Timescales. *Frontiers in Marine Science*, 6(228) doi: 10.3389/fmars.2019.00228

Cheng L., Zhu J., Cowley R., Boyer T., Wijffels, S. (2014) Time, probe type, and temperature variable bias corrections to historical expendable bathythermograph observations. *Journal of Atmospheric and Oceanic Technology*, 31:1793–1825. doi:10.1175/JTECH-D-13-00197.1.

Chiswell, S.M., Bostock, H.C., Sutton, P.J.H., Williams, M.J.M. (2015) Physical oceanography of the deep seas around New Zealand: a review. *New Zealand Journal of Marine and Freshwater Research*. http://dx.doi.org/10.1080/00288330.2014.992918

Cowley R., Wijffels S., Cheng L., Boyer, T., Kizu, S. (2013) Biases in expendable bathythermograph data: a new view based on historical side-by-side comparisons. *Journal of Atmospheric and Oceanic Technology,* 30: 1195–1225. doi:10.1175/JTECH-D-12-00127.1.

Dong, S., Hautala, S.L., Kelly, K.A. (2007) Interannual variations in upper-ocean heat content and heat transport convergence in the western North Atlantic. *Journal of Physical Oceanography,* 37(11): 2682–2697.

Fernandez, D., Bowen, M., Sutton, P. (2018) Variability, coherence and forcing mechanisms in the New Zealand ocean boundary currents. *Progress in Oceanography,* 165: 168-188. https://doi.org/10.1016/j.pocean.2018.06.002

Fernandez, D., Sutton, P., Bowen, M. (2017) Variability of the subtropical mode water in the Southwest Pacific. *Journal of Geophysical research, Oceans,* 122: 7163–7180. doi:10.1002/2017JC013011.

Georgi, D.T., Dean, J.P., Chase, J.A. (1980) Temperature calibration of expendable bathythermographs. *Ocean Engineering,* 7: 491–499.

Hanawa, K., Rual, P., Bailey, R.J., Sy, A., Szabados, M. (1995) A new depth-time equation for Sippican or TSK T-7, T-6 and T-4 expendable bathythermographs (XBT). *Deep Sea Research Part I: Oceanographic Research Papers*, 42: 1423–1451.

Hanawa, K., Talley, L. (2001) Ocean circulation and climate—Observing and modelling the global ocean; Chapter 5.4 Mode waters. *International Geophysics,* 77: 373–386.

Hersbach, H., Bell, B., Berrisford., P., et al. (2020) The ERA5 global reanalysis. *Quarterly Journal of the Royal Meteorological Society,* 2020(146): 1999– 2049. https://doi.org/10.1002/qj.3803

Iselin, CO'D. (1939) The influence of vertical and lateral turbulence on the characteristics of the waters at mid-depths. *Eos, Transactions American Geophysical Union,* 20(3): 414–417.

Kelly, K.A., Small, R.J., Samelson, R.M., Qiu, B., Joyce, T.M., Kwon, Y., Cronin, M.F. (2010) Western Boundary Currents and frontal air–sea interaction: Gulf Stream and Kuroshio Extension. *Journal of Climate,* 23(21): 5644–5667.

McCartney, M.S. (1982) The subtropical recirculation of mode waters. *Journal of Marine Research*, 40: 427–464.

Oke, P.R., Pilo, G.S., Ridgway, K., Rykova, T. (2019) A search for the Tasman Front. *Journal of Marine Systems*, 199. https://doi.org/10.1016/j.jmarsys.2019.103217.

Qiu, B., Hacker, P., Chen, S., Donohue, K.A., Watts, D.R., Mitsudera, H., Hogg, N.G., Jayne, S.R. (2006) Observations of the Subtropical Mode Water evolution from the Kuroshio Extension System Study. *Journal of Physical Oceanography,* 36(3): 457–473.

Rainville, L., Jayne, S.R., Cronin, M.F. (2014) Variations of the North Pacific Subtropical Mode Water from direct observations. *Journal of Climate,* 27(8): 2842–2860.

Ridgway, K.R., Dunn, J.R. (2003) Mesoscale structure of the mean East Australian Current System and its relationship with topography. *Progress in Oceanography,* 56: 189-222.

Roemmich, D.H. (1983) Optimal estimation of hydrographic station data and derived fields. *Journal of Physical Oceanography,* 13: 1544–1549.

Roemmich, D., Boebel, O., Freeland, H., King, B., Le Traon, P-Y., Molinari, B., Owens, W.B., Riser, S., Send, U., Takeuchi, K., et al. (1998) On the design and implementation of Argo: an initial plan for a global array of profiling floats. International CLIVAR Project Office Report 21, GODAE Report 5. *GODAE International Project Office*, Melbourne, Australia: 32.

Roemmich, D., Cornuelle, B. (1990) Observing the fluctuations of gyre-scale ocean circulation: a study of the subtropical South Pacific. *Journal of Physical Oceanography,* 20: 1919–1934.

Roemmich, D., Gilson, J. (2009) The 2004–2008 mean and annual cycle of temperature, salinity, and steric height in the global ocean from the Argo Program. *Progress in Oceanography,* 82(2): 81–100. https://doi.org/10.1016/j.pocean.2009.03.004.

Roemmich, D., Gilson, J., Davis, R., Sutton, P., Wijffels, S., Riser, S. (2005), Decadal Spinup of the South Pacific Subtropical Gyre. *Journal of Physical Oceanography*, 37: 162-173.

Roemmich, D., Gilson, J., Sutton, P., Zilberman, N. (2016), Multidecadal Change of the South Pacific Gyre Circulation. *Journal of Physical Oceanography*, 46: 1871-1883. DOI: 10.1175/JPO-D-15-0237.1

Roemmich, D., Gilson, J., Willis, J., Sutton, P. Ridgway K. (2005), Closing the time-varying mass and heat budgets for large ocean areas: The Tasman Box. *Journal of Climate,* 18(13): 2330–2343.

Roemmich, D., Sutton, P. (1998) The mean and variability of ocean circulation past northern New Zealand: Determining the representativeness of hydrographic climatologies. *Journal of geophysical research*, 103(C6): 13,041-13,054.

Sloyan, B.M., Ridgway, K.R., Cowley, R. (2016) The East Australian Current and property Transport at 27°S from 2012 to 2013. *Journal of Physical Oceanography,* 46(3): 993–1008. DOI: 10.1175/JPO-D-15-0052.1

Sprintall, J., Roemmich, D., Stanton, B., Bailey, R. (1995) Regional climate variability and ocean heat transport in the southwest Pacific Ocean. *Journal of Geophysical Research*, 100: 15,865-15,871.

Stanton, B.R. (1979) The Tasman Front. *New Zealand Journal of Marine and Freshwater Research,* 13(2): 201-214.

Stanton, B.R., Sutton, P.J.H., Chiswell, S.M. (1997) The East Auckland Current, 1994-95. *New Zealand Journal of Marine and Freshwater Research,* 31: 537-549.

Sutton, P.J.H., Bowen, M. (2014) Flows in the Tasman Front south of Norfolk Island. *Journal of Geophysical research, Oceans,* 119. doi:10.1002/2013JC009543.

Sutton, P.J.H., Bowen, M., Roemmich, D. (2005) Decadal temperature changes in the Tasman Sea. *New Zealand Journal of Marine and Freshwater Research*, 39: 1321–1329.

Sutton, P.J.H, Roemmich, D. (2001) Ocean temperature climate off north-east New Zealand. *New Zealand Journal of Marine and Freshwater Research,* 35: 553–565.

Talley, L.D., Pickard, G.L., Emery, W.J., Swift, J.H. (2011) *Descriptive Physical Oceanography: An Introduction*. Academic, Amsterdam: 555.